OPTIMIZATION OF LOW-TEMPERATURE Zn DIFFUSION FOR GaSb SOLAR CELL STRUCTURES FABRICATION

A.W. Bett, N.N. Faleev*, A.M. Mintairov*, A. Namazov*, O.V. Sulima*, G. Stollwerck

Fraunhofer Institut für Solare Energiesysteme, Oltmannsstr. 5, D-79100 Freiburg, Germany
Phone: (+49) 761-4588257, Fax: (+49) 761-4588250
* A.F.Ioffe Physico-Technical Institute, Polytechnicheskaya 26, 194021 St. Petersburg, Russia
Phone: (+7) 812-2479394, Fax: (+7) 812-2471017

ABSTRACT: Zn diffusion into GaSb from the vapour and liquid phase was studied. Diffusion profiles, providing high photocurrents in (thermo)photovoltaic cells were calculated. The possibility of an AlGaAsSb wide gap window application for GaSb solar cells is discussed.

1. INTRODUCTION

GaSb solar (photovoltaic) cells are of large interest for both photovoltaic and thermophotovoltaic applications.

In order to develop a simple and reproducible method of GaSb cells fabrication, the Zn-diffusion into GaSb was studied in this work.

Computer calculations of diffused emitters, providing high photocurrents were carried out for concentrator GaSb solar cells in GaAs-GaSb tandems. The results of these calculations show the strong dependence of the solar cell photocurrent on Zn-profiles in the GaSb cell structure.

Two methods of Zn-diffusion were experimentally investigated in this work: (a) diffusion from the vapour phase in a pseudo-closed box system and (b) diffusion from the liquid phase from a Ga-Zn based melt. Quite different Zn profiles were obtained in these two cases. However, the advantages of both approaches can be used in a cell fabrication process. Moreover, first experiments on the liquid phase epitaxy (LPE) growth of a AlGaAsSb wide gap window, lattice matched to the GaSb substrate, show the possibility of the epitaxy-diffusion combination in a simple one-melt LPE boat.

2. SIMULATION WITH PC-1D

The structure of a diffused emitter in a GaSb wafer with a base doping of $3\,10^{17}$ cm^{-3} was modelled using PC-1D[1]. As modelling parameters, the surface concentration of ionized acceptors (N_A) was varied in the range of $5\,10^{17}$ to $5\,10^{21}$ cm^{-3} and the emitter thicknesses in the range of 30 nm to 2 µm. The semiconductor parameters used for the simulation are listed below.

Intrinsic parameters: $n_i(300K)= 1.5\,10^{11}$ cm^{-3}, $N_C/N_V= 0.558$, calculated from [2];
Electron mobility: $\mu_{max}= 1.8\,10^4$ cm^2/Vs, $\alpha= 0.68$, $N_{ref}= 4.5\,10^{17}$ cm^{-3} [3];
Hole mobility: $\mu_{max}= 1.9\,10^3$ cm^2/Vs, $\alpha= 0.33$, $N_{ref}= 5.8\,10^{16}$ cm^{-3} [4,5];
Surface recombination: $S_{front}= 10^4$ cm/s, $S_{back}= 10^7$ cm/s;
Auger recombination: $C_{ph}= 4\,10^{-30}$ cm^6/s [6];
Radiative recombination: $B_p= 5\,10^{-11}$ cm^3/s [6];
SRH lifetime: $\tau_n = 2$ nsec, $\tau_p = 10$ nsec [6].
Band gap narrowing was taken into account according to Ref. [7].

Fig.1 shows the calculated short-circuit currents (I_{SC}) of a GaSb cell under a GaAs filter (AM1.5D, 200 suns) in dependence on the diffused emitter thickness and the surface concentration of ionized acceptors. One can see that the highest values of I_{SC} can be obtained for low values of N_A at the surface. In this case, the emitter thickness can be relatively large, up to 2.0 µm. For higher N_A values much thinner emitters are necessary. However, thin emitters are not favourable for the cell technology.

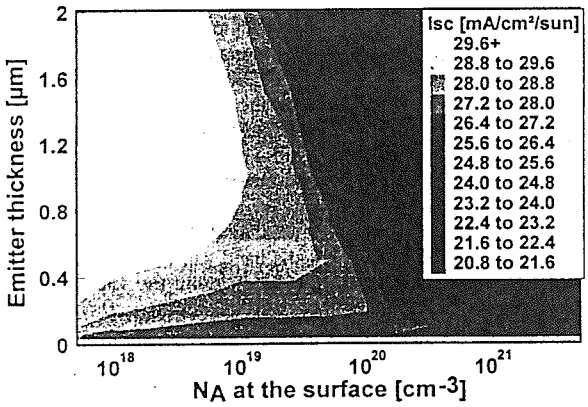

Figure 1: Calculated short-circuit current (Isc) of a GaSb cell under a 300 µm thick GaAs filter in dependence on the diffused emitter thickness and on the surface concentration of ionized acceptors.

3. EXPERIMENTAL DETAILS

Zn-diffusion from the vapour phase was performed into n-GaSb:Te substrates in a pseudo-closed box system similar to that described in Ref. [8]. However, a modification of the graphite diffusion boats, used in [8], was made. The new multi-wafer boat allows (i) to place wafers vertically or horizontally in the same boat, (ii) to vary the distance between the wafers with a minimum distance of 0.5 mm, (iii) to use different vapour sources (pure Zn or Zn and Sb, not mixed) and (iv) to increase the wafer area up to 4x4 cm^2. A special design of the graphite boat for Zn diffusion ensured the uniformity of the Zn vapour pressure across the wafer surface, and thus the uniformity of the p-GaSb layer depth. Zinc and antimony were always used in more than sufficient quantities to provide saturation vapour pressures. Relatively low temperatures of diffusion (450-520°C) were used for diffusion from the vapour phase. The diffusion time was 1 hour.

Zn-diffusion from the liquid phase was performed in a simple one-melt slider-type LPE boat at T=530-555°C. Two types of such diffusion processes were investigated: An etchback-diffusion process and a growth-diffusion process. In the case of the etchback - diffusion process, the Ga-Zn based melt, undersaturated with Sb,

partially dissolves the GaSb substrate. After that the isothermal Zn diffusion into GaSb takes place. At the end of the process the melt is removed from the surface. In the case of the growth-diffusion process, a supersaturated (with respect to Sb) Al-Ga-As-Sb-Zn melt is brought into contact with a GaSb substrate. This results in the growth of a several μm thick AlGaAsSb layer and in the formation of a diffused p-GaSb layer under it. The contact (diffusion) time was 1-2h. In some experiments a slow cooling rate (0.08°/min) of the system was used during the contact time. The process was terminated by removing the melt from the substrate.

4. CHARACTERIZATION OF DIFFUSED LAYERS

4.1 Diffusion from the vapour phase

The diffused p-GaSb layers were characterized by secondary ion mass spectroscopy (SIMS), Raman scattering spectroscopy and x-ray rocking curve method. Zn-atom and hole concentration profiles of p-GaSb layers were determined by the method of Zn diffusion (from the vapour or liquid phase). Moreover, their dependence on the distance between substrates as well as on the vapour pressure of Sb in the boat was observed for the diffusion from the vapour phase.

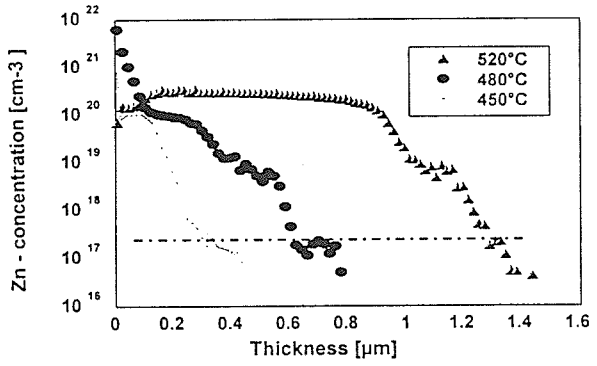

Figure 2: Zn concentration profiles after diffusion of Zn from the vapour phase at different temperatures for 0.5 mm distance between the wafers with the presence of Sb. The dash dot line shows the doping level in the n-GaSb:Te substrate.

Fig. 2 shows the SIMS profiles of Zn concentration after diffusion from the vapour phase at different temperatures. It is noteworthy that essential changes in Zn concentration take place near the surface of the wafer depending on the temperature. At a temperature of 480°C the highest surface concentration is measured. At the lower temperature the Zn vapour pressure is not high enough to provide the maximum Zn concentration in GaSb. At the higher temperature an erosion of GaSb surface takes place leading to a decrease of the surface concentration.

The x-ray studies of the same p-GaSb layers were performed with a double-crystal x-ray diffractometer configured in the (400) geometry using a Ge asymmetrically cut monochromator crystal. Fig.3 demonstrates the difference in x-ray rocking curves of the samples with the Zn profiles shown in Fig.2. With higher temperature the rocking curve becomes assymetrical and broader. At 520°C a separate peak appears. These changes correspond to the increase of the Zn concentration and the emitter thickness. A decrease of the lattice parameter $\Delta a \approx 2\,10^{-3}$ Å in the diffused layers in comparison with the substrates was measured.

Fig.4 shows the SIMS profiles of Zn concentration after diffusion from the vapour phase at different distances between the wafers with and without Sb in the boat. One can see that both, increasing the distance between the wafers and adding Sb, decrease the penetration of Zn into the substrate. If one assumes the similar dependence of the Zn-diffusion in GaSb on the vapour pressure of B^5-element as in GaAs [9], the difference in the diffusion profiles can be explained by different conditions for Sb desorption from the GaSb surface. The larger the distance between the wafers, the stronger is the desorption of Sb and the more Zn penetrates into GaSb. Addition of Sb into the boat decreases the Sb desorption due to the higher vapour pressure of pure Sb in comparison with the pressure over the GaSb surface.

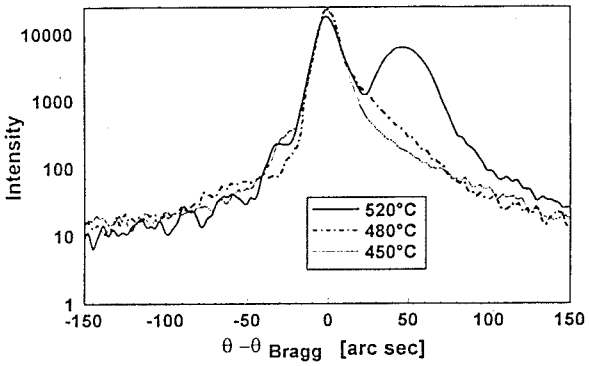

Figure 3: X-ray rocking curves of the samples with the Zn concentration profiles shown in Fig.2

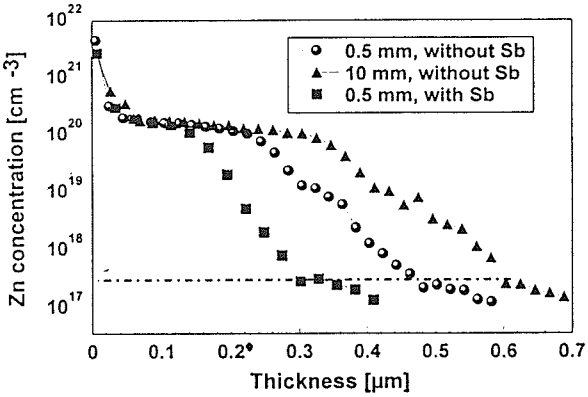

Figure 4: Zn concentration profiles after Zn-diffusion from the vapour phase at 450°C for different distances between the wafers with and without Sb. The dash dot line shows the doping level in the n-GaSb:Te substrate.

Free-hole profiles in p-GaSb were measured by Raman-spectroscopy. The depth resolution was provided by a precise layer-by-layer anodic oxidation of GaSb and corresponding selective etching of the oxide. The details of these measurements are described in Ref. [8]. One of the Raman scattering free-carrier profiles together with the SIMS Zn profile is shown in Fig.5.

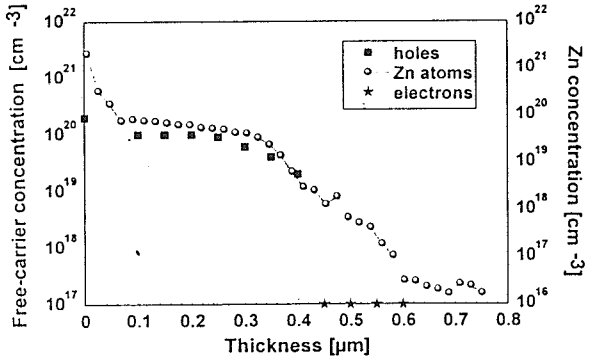

Figure 5: Raman scattering free-carrier profiles and SIMS Zn profile of the GaSb structure after diffusion of Zn from the vapour phase at 450°C (10 mm distance between wafers, without Sb).

The coincidence of the SIMS and Raman spectroscopy measurements for the Zn (hole) concentrations between 10^{19}-10^{20} cm^{-3} is quite good. That means that almost all Zn atoms are electrically active in that part of the diffused layer.

4.2 Diffusion from the liquid phase

Fig.6 shows the SIMS Zn concentration profile in GaSb:Te after the diffusion at 554°C (2h) from a Ga-0.3at%Zn based melt. This profile exhibits much smaller surface concentration than in the case of diffusion from the vapour phase, thus meeting the demands of the PC-1D simulation for the "high-photocurrent" emitter. In this case no epitaxial layer was grown. However, a high temperature stability of the process should be provided in this case: Small temperature fluctuations may cause an uncontrolled dissolution of the diffused layer or an epitaxial growth.

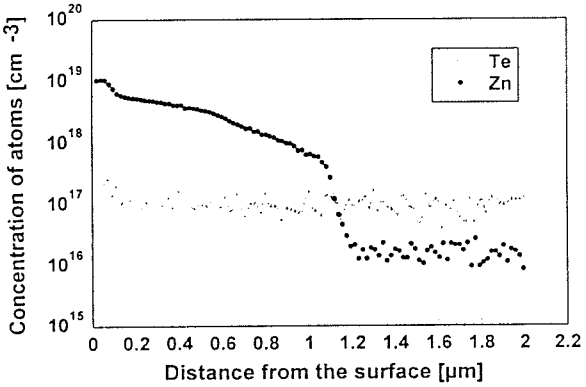

Figure 6: Zn and Te (substrate dopant) profiles after diffusion of Zn from the liquid phase at 554°C from a Ga-0.3at%Zn based melt.

Taking into account our experience in the field of Zn diffusion in AlGaAs-GaAs system [10], we suppose that more reproducible diffusion from the liquid phase could be performed through an Al-containing A^3B^5 epilayer with a wider bandgap than GaSb. In this case, small fluctuations of temperature in the melt during diffusion time may change the epitaxial but not the diffusion layer. Moreover, such an epitaxial layer could act as a wide gap window passivating the GaSb cell. Unfortunately, AlGaSb is not the best candidate for such a window layer. The relatively large difference in lattice parameters of AlGaSb and GaSb prevents the formation of a uniform AlGaSb transient layer in the melt-substrate system and causes an extremely nonuniform dissolution of the GaSb substrates during the etchback-regrowth process (Fig.7). This dissolution happens even with supersaturated (with respect to antimony) melts. However, addition of a small amount of arsenic into the melt changes the situation drastically and results in a growth of high-quality lattice-matched AlGaAsSb layers (Fig.8). This was proved by x-ray rocking curve measurements. One should note that the epitaxial growth and diffusion can take place simultaneously and therefore, be performed during one technological run.

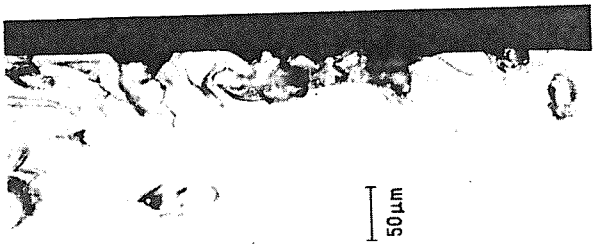

Figure 7: Photograph of the anodically oxidized cross-section of the AlGaSb-GaSb(substrate) structure. Rests of the melt are visible at the bottom of the dissolution channels.

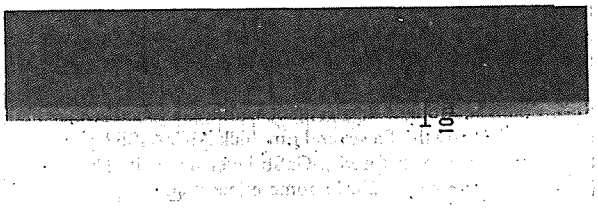

Figure 8: Photograph of the anodically oxidized cross-section of the lattice-matched AlGaAsSb-GaSb(substrate) structure.

GaSb CELLS AND PHOTOVOLTAIC MEASUREMENTS

0.4 x 0.4 cm^2 and 1x1cm^2 solar cells were fabricated on the structures with a diffused emitter. Up to now, only diffusion from the vapour phase was used for fabrication of the cells. One should note several peculiarities of the cell design. First (in the case of 0.4 x 0.4 cm^2 cells), the diffused layer was formed locally with the help of a diffusion mask. Second, in order to decrease the metal-semiconductor contact area and the effective surface recombination velocity, the contact busbar was deposited mainly on the SiN mask. Both approaches resulted in a low reverse diode current of the solar cell: 0.6 mA/cm^2 at 0.7 V for the cell with the 0.2 µm thin emitter under the contacts. In order to reduce the influence of the metal-semiconductor interface recombination on the open-circuit voltage, one should increase the thickness of the diffused layer only under the contact grid. We have determined experimentally that it should be thicker than 0.5 µm. Fig.1 showed that much thinner emitters are favourable for the high photocurrent, if the high Zn concentrations typical for diffusion from the vapour phase are taken into account. Therefore, at the final stage of solar cell fabrication, the 0.5-1.0 µm thick emitter was made thinner between the grid fingers. This thinning was performed by anodic oxidation and corresponding selective etching of the anodic oxide. As a result, a two-step emitter structure was fabricated. The anodic oxide was also used as an antireflection coating (ARC). The schematical cross-section of this structure is shown in Fig. 9.

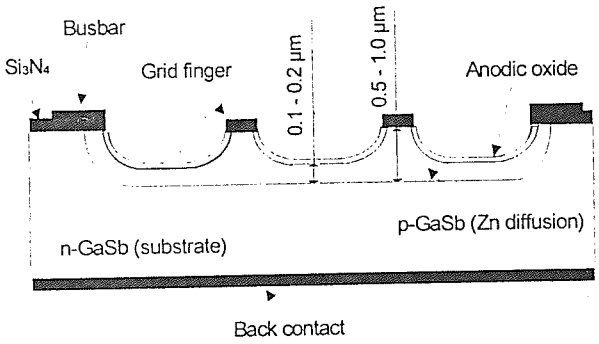

Figure 9: Schematical cross-section of a GaSb cell with local diffusion and local emitter thinning.

The typical spectral response and reflectivity curves for GaSb solar cell with ≈ 0.1 µm thin emitter (between grid fingers) and 0.14 µm anodic oxide ARC are shown in Fig. 10. The spectral response was quite uniform across the wafer and should correspond to a high photocurrent. However, some additional steps should be undertaken in order to perform exact photocurrent measurements. Nevertheless, even now the results of the solar cell measurements are quite promising:

1. A high external efficiency (≈ 80%) was measured in the wavelength region 800-1650 nm. Taking into account the reflectance spectrum, this corresponds to more than 90% internal quantum efficiency of the fabricated solar cells in this region.
2. An open-circuit voltage of nearly 0.5 V was achieved for the light intensity corresponding to approximately 100 suns.

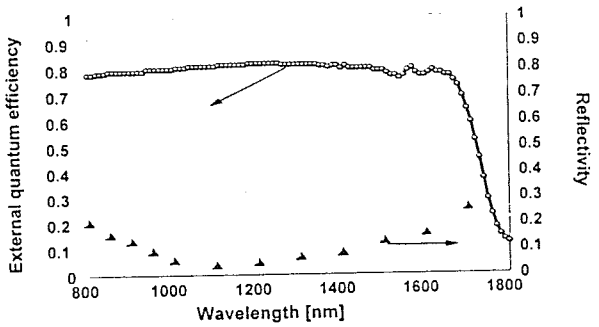

Figure 10: IR-part of spectral response and reflectivity of the GaSb solar cell with ≈ 0.1 μm thin emitter and 0.14 μm anodic oxide ARC.

Taking into account our results of the characterization of diffused layers, one can suppose that a two-step Zn diffusion might be useful. First, a "deep" diffusion from the liquid phase will result in the diffusion profile with a low surface concentration. This profile is favourable for high I_{sc} values. Second, an additional "shallow" diffusion from the vapour phase will result in formation of a very thin surface layer (< 10 nm) with a high concentration. This surface layer is favourable for reduction of the contact resistance without reduction of the photocurrent. Such approach was succesfully used for AlGaAs-GaAs solar cells [11].

5. CONCLUSIONS

PC-1D simulation has shown that the highest photocurrent in GaSb cells can be obtained for 0.5-2.0 μm thick diffused emitters with low surface N_A values (around 10^{18} cm^{-3}).

For Zn-diffusion from the vapour phase high surface Zn concentrations (>10^{21} cm^{-3}) are typical. Zn-profiles are dependent on the method of diffusion (from the vapour or liquid phase), diffusion temperature, distance between substrates, vapour pressure of Sb in the diffusion boat.

A surface Zn concentration in the range of 10^{19} cm^{-3} has been achieved by diffusion from the liquid phase. Combination of such diffusion with the epitaxial growth of a lattice matched AlGaAsSb wide gap window layer is possible.

6. ACKNOWLEDGEMENTS

The authors wish to thank Dr. B. Ber and his coworkers for SIMS measurements, Dr. P. Lanyi for x-ray measurements of AlGaAsSb layers, A. B. Kazantsev for spectral response measurements, Prof.-Dr. V.M. Andreev and Prof.-Dr. W. Wettling for helpful discussion of the results.

REFERENCES

[1] PC-1D, Version 3, P. Basore, Sandia Nat. Lab., Albuquerque, USA (1991)
[2] Landolt-Börnstein, Num. Data and Func. Relationships in Science and Technology, Vol. 17a III-V Semiconductors, Springer Verlag Berlin (1982)
[3] V.W.L. Chin, Sol. State. Electron., 38 (1995), 59
[4] M.W. Heller, R.G. Hamerly, J. Appl. Phys., 57 (1985), 4626
[5] P.C. Mathur, Sushil Jain, Phys. Rev. B, 19 (1979), 3152
[6] A.N. Titkov, E.I. Chaykina, E.M. Komova, N.G. Ermakova, Sov. Phys. Semicond. 20 (1986), 16
[7] S.C. Jain, J.M. McGregor, D.J. Roulston, J. Appl. Phys., 68 (1990), 3747
[8] O.V. Sulima, N.N. Faleev, A.B. Kazantsev, A.M. Mintairov, A. Namazov, Proceedings 4th European Space Power Conference, ESA Publications Division (1995), v.2, 641
[9] D. Shaw, Atomic Diffusion in Semiconductors, Plenum Press (1973)
[10] A. Baldus, A. Bett, O.V. Sulima, W. Wettling, J.Cryst. Growth, 146 (1995), 299
[11] A. Blug, A. Baldus, A.W. Bett, U. Blieske, G. Stollwerck, O.V. Sulima, W. Wettling, Zn post diffusion for GaAs LPE-ER concentrator solar cells, this Conference.